THE JOURNAL OF BIOLOGICAL CHEMISTRY
Vol. 277, No. 40, Issue of October 4, pp. 37406–37413, 2002

Printed in U.S.A.

Structure of the BgK-Kv1.1 Complex Based on Distance Restraints Identified by Double Mutant Cycles

MOLECULAR BASIS FOR CONVERGENT EVOLUTION OF Kv1 CHANNEL BLOCKERS*

Received for publication, June 21, 2002, and in revised form, July 19, 2002
Published, JBC Papers in Press, July 19, 2002, DOI 10.1074/jbc.M206205200

Bernard Gilquin‡§, Judith Racapé‡, Anja Wrisch¶, Violeta Visan¶, Alain Lecoq‡, Stephan Grissmer¶, André Ménez‡, and Sylvaine Gasparini‡§

From the ‡Département d'Ingénierie et d'Etudes des Protéines, CEA Saclay, 91191 Gif sur Yvette cedex, France and the ¶Department of Applied Physiology, University of Ulm, Albert-Einstein-Allee 11, 89081 Ulm, Germany

A structural model of BgK, a sea anemone toxin, complexed with the S5-S6 region of Kv1.1, a voltage-gated potassium channel, was determined by flexible docking under distance restraints identified by a double mutant cycles approach. This structure provides the molecular basis for identifying the major determinants of the BgK-Kv1.1 channel interactions involving the BgK dyad residues Lys^{25} and Tyr^{26}. These interactions are (i) electrostatic interactions between the extremity of Lys^{25} side chain and carbonyl oxygen atoms of residues from the channel selectivity filter that may be strengthened by solvent exclusion provided by (ii) hydrophobic interactions involving BgK residues Tyr^{26} and Phe^{6} and Kv1.1 residue Tyr^{379} whose side chain protrudes in the channel vestibule. In other Kv1 channel-BgK complexes, these interactions are likely to be conserved, implicating both conserved and variable residues from the channels. The data suggest that the conservation in sea anemone and scorpion potassium channel blockers of a functional dyad composed of a lysine, and a hydrophobic residue reflects their use of convergent binding solutions based on a crucial interplay between these important conserved interactions.

Although most biological processes are governed by protein-protein recognition phenomena, the molecular determinants of the specificity of these interactions are yet poorly understood. In particular, one protein ligand can bind multiple receptors and a receptor can be bound by several protein ligands of similar or even different structures (l-3), and the molecular mechanisms underlying these multiple bindings are not well understood. Kv1 voltage-gated potassium channels and toxins from scorpions, snakes, sea anemones, and conus that block currents through these channels offer an appropriate mean to investigate the molecular basis of such pleiotropic aspects of protein-protein interactions. Indeed, a potassium channel can be blocked by different toxins of similar or different folds, and conversely a toxin can bind to several members of Kv1 channels (3). Two lines of evidence suggest that the four groups of toxins use a convergent solution to block Kv1 channels. First, despite their unrelated structures, they all exert their function by binding to the same P-region of the channels, comprised between transmembrane segments S5 and S6 (4–12). Second, the binding sites of all these toxins contain a functional dyad composed of a lysine and a hydrophobic residue that might constitute a minimal functional core for the toxins to bind Kv1 channels, whereas additional residues might provide each toxin with a specific binding profile (3, 13–17).

To get further insights into the toxin-channel interactions and in particular into the role of the dyad residues, we used double mutant cycle analysis to identify proximities between residues of BgK, a sea anemone toxin, and Kv1.1. Then, these proximities were used to determine the structure of BgK complexed with the S5-S6 region of Kv1.1. Analysis of this model provides a molecular basis for the convergent evolution of toxins that block Kv1 channels.

EXPERIMENTAL PROCEDURES

Materials—BgK as well as the analogs were synthesized using a previously described procedure (13). α-DTX[1] and BgK(W5Y/Y26F) were iodinated as described in Ref. 18. The cDNA encoding mKv1.1 and mKv1.3 were generously provided by Dr. George K. Chandy, (University of California, Irvine, CA). The cDNA encoding hKv1.6, cloned into the mammalian expression vector pcDNA3 (Invitrogen), was kindly provided by Prof. Olaf Pongs (Zentrum für Molekulare Neurobiologie, Hamburg, Germany). Mutagenesis was made using the PCR technique (QuickChange™ site-directed mutagenesis kit, Stratagene) and mutations were confirmed by sequencing.

Production of Kv1 Channels in RBL Cells—Culture of RBL cells, linearization of plasmids, *in vitro* transcription, and injections were carried out as described previously (19).

Electrophysiological Recordings—All recordings were carried out using the whole-cell recording mode of the patch clamp technique as described previously (19, 20).

Binding Assays—Heterologous expression of hKv1.1, hKv1.2, and hKv1.6 channels in mammalian cells, binding experiments, and data analysis were carried out as described in Ref. 18.

Modeling of the Kv1.1 S5-S6 Region—The sequence identity between the S5-S6 region of Kv1.1 (residues 325–409) and region 28–112 of KcsA is 32%. For the region comprised between the two transmembrane segments S5 and S6, the sequence identitiy is 47% between both channels (Kv1.1, residues 348–382; KcsA, residues 51–85). Based on this high degree of similarity, a model of the S5-S6 region of Kv1.1 was generated by Modeler 4.0 (21), using the recently solved structure of the potassium channel of *Streptomyces lividans* (22) (Protein Data Bank

* This work was supported by grants from the Deutsche Forschungsgemeinschaft (Gr 848/8.2) and the Bundesministerium für Bildung und Forschung (both grants to S. Grissmer). The costs of publication of this article were defrayed in part by the payment of page charges. This article must therefore be hereby marked "*advertisement*" in accordance with 18 U.S.C. Section 1734 solely to indicate this fact.

§ To whom all correspondence may be addressed: DIEP, Bât 152, CEA Saclay, 91191 Gif sur Yvette cedex, France. Tel.: 33-1-69-08-35-88 (for S. Gasparini) or 33-1-69-08-30-26 (for B. Gilquin); E-mail: gasparin@dsvidf.cea.fr or bgilquin@cea.fr.

[1] The abbreviations used are: DTX, dendrotoxin; HEK, human embryonic kidney; RBL, rat basophilic leukemia; r.m.s.d., root mean square deviation; wt, wild type; mut, mutant.

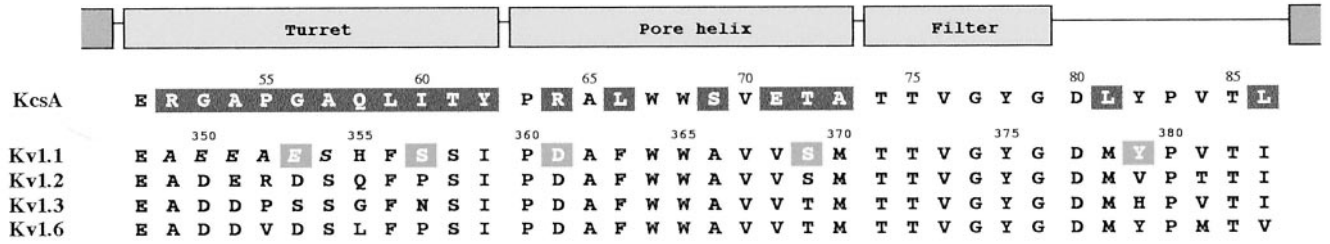

FIG. 1. **Alignment of the amino acid sequences of the P-region of KcsA and Kv1 channels.** Residues differing between KcsA and Kv1.1 are indicated in *black boxes* in the KcsA sequence. Residues of Kv1.1 that were substituted for the double mutant cycle analysis are indicated in *gray boxes*.

code 1K4C) as template. The resulting model displays a Cα r.m.s.d. to the original x-ray structure of KcsA equal to 0.5 Å and 0.26 Å for all the structure and the most conserved region (selectivity filter: TTVGYGD), respectively. Structures of the complex BgK-Kv1.1 were calculated by high temperature molecular dynamics simulation and minimization under NMR-style distance restraints (23) derived from experimental results. The minimized average structure of BgK (13) was manually positioned above the channel pore with its functional site (Ref. 24 and Fig. 5) facing the entrance of the pore. To explore systematically the different positions of the toxin on the channel, 400 complex structures were calculated by rotating the toxin around the pore axis. A rigid body simulated annealing procedure at 5,000 K (1,000 steps), then at 500 K (1,000 steps), was used to dock BgK on Kv1.1, driven by six distance restraints of 6 + 1, −3 Å between the residues (BgK-Kv1.1): $Phe^{6}(C\epsilon)$-$Tyr^{379}(C\epsilon)$, $Asn^{19}(N\delta2/O\delta1)$-$Ser^{357}(O\gamma)$, $Ser^{23}(O\gamma/H\gamma)$-$Tyr^{379}(C\epsilon)$, $Tyr^{26}(C\epsilon/O\eta)$-$Ser^{357}(O\gamma)$, $Tyr^{26}(C\epsilon/O\eta)$-$Asp^{361}(O\delta)$, and $Tyr^{26}(C\epsilon/O\eta)$-$Tyr^{379}(C\epsilon)$ with no assignment of the channel subunit. The potassium ions in the S3 site and in the cavity as well as the water molecule in the S4 site and those in the cavity (22, 25, 26) were explicitly included.

The 49 energetically best complexes were refined, using a procedure in which the structure of BgK was progressively relaxed by decreasing harmonic restraints from 1,000 to 0 kcal/mol/Å^2 to allow flexibility of the side chains. Fluctuations in the turret regions of Kv1.1 were permitted by applying no harmonic restraints on residues 349–361. To ensure continuity between the turrets and the other parts of the channel, harmonic restraints of 5 kcal/mol/Å^2 were applied to the atoms of residues 346–348 and 362–364. The rest of the channel was maintained fixed by applying harmonic restraints of 1,000 kcal/mol/Å^2. The procedure included 5,000 steps of dynamics at 500 K and 8,000 steps of dynamics at 400 K using 0.8-fold reduced Van der Waals radii, followed by 10,000 steps at 300 K, using classical Van der Waals radii, under harmonic restraints. Then, 2,000 steps of minimization were performed. The 10 best structures were examined and for each restraint, and the closest channel subunit was chosen. Last, these structures were minimized with a dielectric constant equal to 10 under the following modified distance restraints: 6 + 1, −3 Å between the residues (BgK-Kv1.1 subunit) (subunits were named clockwise A, B, C, and D): Phe^{6} (cycle atoms)-$Tyr^{379}{}_{A}$ (cycle atoms), $Asn^{19}(N\delta2/O\delta1)$-$Ser^{357}{}_{C}(O\gamma)$, $Ser^{23}(O\gamma/H\gamma)$-$Tyr^{379}{}_{D}(O\eta)$, $Tyr^{26}(O\eta)$-$Ser^{357}{}_{D}(O\gamma)$, $Tyr^{26}(O\eta)$-$Asp^{361}{}_{D}$ ($O\delta$) and Tyr^{26}(cycle atoms)-$Tyr^{379}{}_{D}$(cycle atoms). Nonbonded interactions were calculated with a switching function extending from 7.5 to 9.0 Å. A united atom model was used in which nonpolar hydrogen atoms attached to carbon atoms are incorporated into the latter, but the polar hydrogen atoms were treated explicitly. All the calculations were carried out using X-PLOR (27) in a force field derived from CHARMM19 (file topallh19.pro and parallh19.pro in X-PLOR 3.1). Van der Waals and electrostatic energies for all the residues-residues pairs were calculated, and residues were considered as interacting for energies >1 kcal·mol^{-1}.

RESULTS

Double Mutant Cycles—For each cycle of the double mutant analysis, the effect of a substitution in BgK on the effect of a substitution in Kv1.1 was quantified by measuring the affinity of wild-type and monosubstituted BgK for wild-type and monosubstituted mKv1.1 channels. Choice of residues substituted in BgK was based on previous results (24); three residues reported as important for binding to Kv1.1 (Asn^{19}, Lys^{25}, and Tyr^{26}) and two reported as less or not important (His^{13} and Phe^{6}) were substituted by alanine. In the P-region of Kv1.1, four positions, reported to be important for toxins binding (28–30), were individually mutated: two residues from the turret (Glu^{353} and Ser^{357}) and one from the loop connecting the selectivity filter to the second trans-membrane-helix (Tyr^{379}) were substituted by the corresponding ones in Kv1.3, and residue Asp^{361} from the pore helix was substituted by an asparagine residue (Fig. 1). As a control, we also substituted a buried residue from the pore helix (S369T). The electrophysiological properties of the mutant channels in respect to the voltage dependence of activation, deactivation, and inactivation were not significantly different from wild-type channels. Minor changes in respect to the time course of inactivation were observed as expected, for example for the Y379H mutant channel (for comparison, see Ref. 31). Since toxin affinity was estimated using changes in peak current amplitudes, minor changes in the inactivation time course will not influence these estimations.

The analogs of BgK were first tested both by electrophysiological and binding experiments (Fig. 2, *A* and *B*) on wild-type Kv1.1. For electrophysiological experiments, analogs F6A, H13A, N19A, and Y26A were tested by dose-response experiments (Fig. 2*A*), whereas K_d values for analogs W5A, S23A, Q24A, and K25A were deduced from the block of current by certain concentrations that allowed the calculation of K_d values assuming a 1:1 stoichiometry. All the values are shown in Table I. Probably reflecting differences in the state of the channels used in both experiments, the affinity of BgK for Kv1.1 measured in electrophysiological experiments is nanomolar, whereas it is picomolar in binding experiments. However, despite this affinity range difference, the effects of substitutions on both the capacity of BgK to block current through Kv1.1 channels and to inhibit ^{125}I-α-DTX binding to Kv1.1 channels were found to be similar (Fig. 2*C*) and in the same range than those reported in a previous study (24). All the values are shown in Table I. Then, the affinity of wild-type BgK was measured for the five mutated channels; results indicate that both the turret (mutations E353S and S357N) and the loop connecting the selectivity filter to the second trans-membrane helix (mutation Y379H) are important for BgK binding to Kv1.1 channel (Fig. 2*D* and Table I).

Double mutant cycles were carried out for the five analogs of BgK and the five Kv1.1 mutants. In addition, since a preliminary model of the complex BgK-Kv1.1 suggested proximities between residues Trp^{5}, Ser^{23}, and Gln^{24} from BgK and residue Tyr^{379} from Kv1.1, we also made cycles for these residues. All the K_d values are reported in Table I. The coupling energy $\Delta\Delta G$ values (in kcal·mol^{-1}) (32, 33), which measures the co-operativity of the effects of substitutions in both BgK and the channel, was calculated using the following equation: $\Delta\Delta G = RT \ln [K_d \text{ (wt, wt)}. K_d \text{ (mut, mut)}]/[K_d \text{ (wt, mut)}\cdot K_d \text{ (mut, wt)}]$ (R = 1.99 cal·mol^{-1} and T = 293 K) are

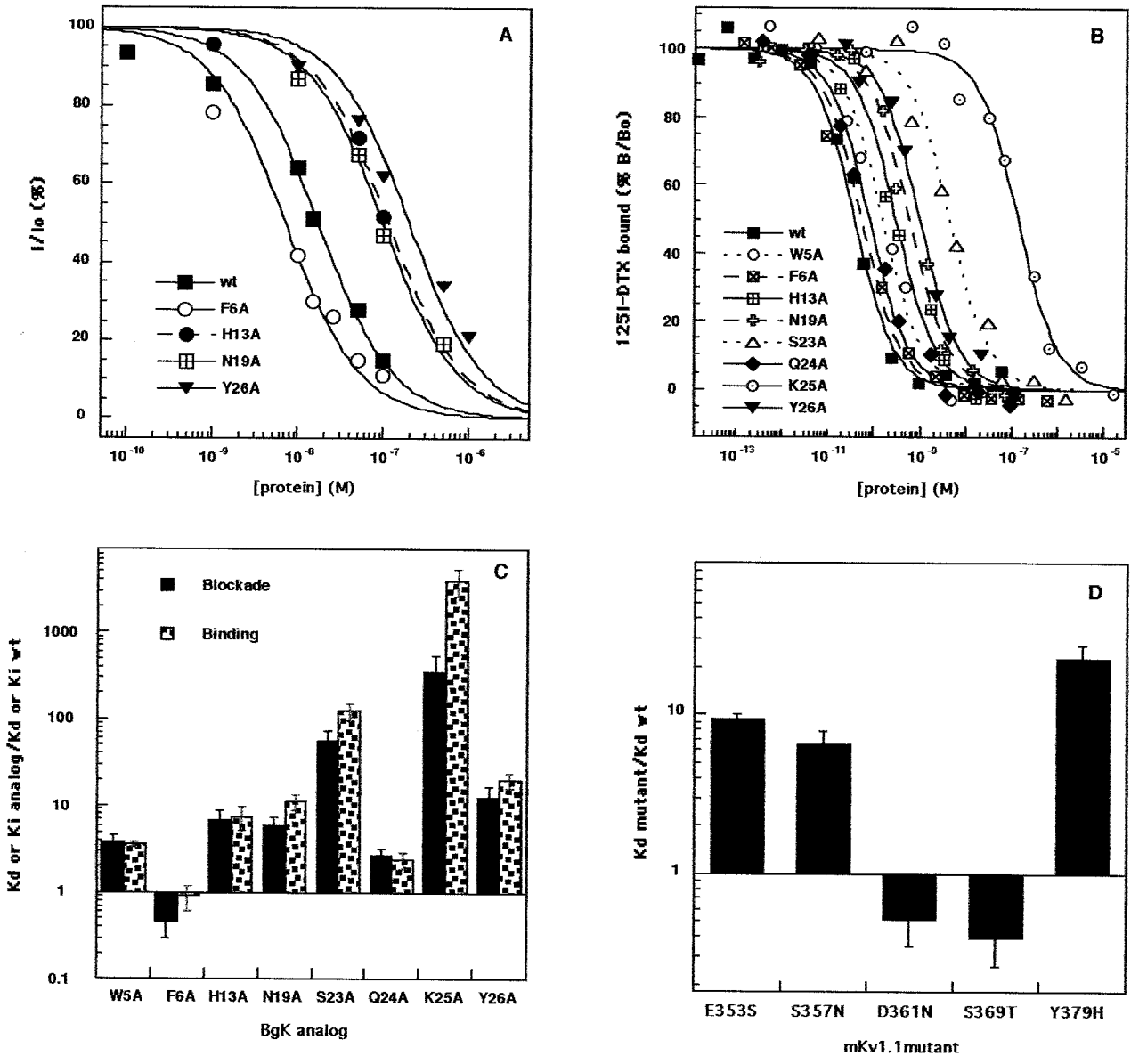

FIG. 2. **Affinity of BgK and BgK analogs for Kv1.1 and mutants of Kv1.1.** *A*, dose-response curves of BgK peptides to block current through mKv1.1 expressed in RBL cells. Each point corresponds to the mean value of three to seven experiments. Data were fitted with the Hill equation with the Hill coefficient fixed to 1. *B*, membranes prepared from HEK-293 cells producing hKv1.1 were incubated with 10 pM ^{125}I-α-DTX in the absence or presence of increasing concentrations of BgK peptides. Inhibition of binding was assessed relative to an untreated control. *C*, comparison of the effects of alanine substitutions in BgK on affinity for Kv1.1 measured either by binding experiments or by electrophysiological experiments. *D*, effects of substitutions in mKv1.1 on the affinity of BgK measured by electrophysiology.

reported in Table I and displayed in Fig. 3, they vary between 0.08 kcal·mol^{-1} for H13A-E353S or F6A-S357N (BgK-Kv1.1) to 2.33 kcal·mol^{-1} for K25A-Y379H.

Model of the Complex BgK/S5-S6 Region of Kv1.1—The complexes were calculated using high temperature molecular dynamics simulation and minimization under distance restraints, as deduced from coupling energies. Indeed, it has been shown that these coupling energies may reflect proximity between residues (33, 34); in an extensive study for validating the signification of coupling energies (34), it was found that values >0.6 kcal·mol^{-1} were determined for residues separated by less than 5 Å. In our study, we found a value of coupling energy up to 0.73 kcal·mol^{-1} for a cycle, implicating a buried residue of the channel (Ser^{369}) used as a negative control. Therefore, we used as a threshold the value of 0.7 kcal·mol^{-1} for interpreting coupling energies as proximity between the mutated residues. Furthermore, coupling energies reflect proximities, provided the substitutions have not induced any structural rearrangement (33, 34). Since the critical substitution K25A in BgK was coupled to all the channel substitutions, even when the residue was buried (Ser^{369}) (Table I), we suspected a nonspecific effect due to a structural rearrangement at the complex interface. Therefore, no distance restraint was applied on residue Lys^{25}. By contrast for all the other residues for which several double mutant cycles were achieved, both kind of coupling energies values were determined: > or <0.7 kcal·mol^{-1}. Thus, coupling energies higher than 0.70 kcal·mol^{-1} were considered to reflect a distance restraints of 6 + 1, −3 Å, which was therefore applied to the following pairs of residues in the BgK-Kv1.1 complex: Phe^{6}-Tyr^{379}, Asn^{19}-Ser^{357}, Ser^{23}-Tyr^{379}, Tyr^{26}-Ser^{357}, Tyr^{26}-Asp^{361} and Tyr^{26}-Tyr^{379} (see "Experimental Procedures").

TABLE I
Double mutant cycle analysis
Dissociations constants of BgK and BgK analogs on Kv1.1 and Kv1.1 mutants and coupling energies ($\Delta\Delta G$).

	Kv1.1 wt, K_d (nM) ± 2 S.E. (*n*)	Kv1.1 E353S		Kv1.1 S357N		Kv1.1 D361N		Kv1.1 S369T		Kv1.1 Y379H	
		K_d (nM) ± 2 S.E. (*n*)	$\Delta\Delta G$ (*kcal·mol*$^{-1}$)	K_d (nM) ± 2 S.E. (*n*)	$\Delta\Delta G$	K_d (nM) ± 2 S.E. (*n*)	$\Delta\Delta G$ (*kcal·mol*$^{-1}$)	K_d (nM) ± 2 S.E. (*n*)	$\Delta\Delta G$ (*kcal·mol*$^{-1}$)	K_d (nM) ± 2 S.E. (*n*)	$\Delta\Delta G$ (*kcal·mol*$^{-1}$)
BgK wt	17 ± 2 (9)[a]	141 ± 8.8 (4)		107 ± 10 (4)		8.4 ± 1.9 (14)		6.4 ± 1.4 (8)		370 ± 38 (4)	
BgK W5A	61 ± 7 (4)[a]	ND[b]	ND	ND	ND	ND	ND	ND	ND	2,013 ± 168 (3)	*0.24*
BgK F6A	7.3 ± 1.8 (5)[a]	42 ± 5.4 (4)	*0.21*	53 ± 4.5 (4)	*0.08*	12 ± 2 (11)	*0.70*	3.9 ± 0.6 (9)	*0.20*	2,830 ± 385 (5)	*1.67*
BgK H13A	109 ± 21 (5)[a]	1,038 ± 22 (4)	*0.08*	888 ± 62 (3)	*0.15*	97 ± 22 (5)	*0.34*	57 ± 6 (6)	*0.19*	1,100 ± 68 (4)	*0.44*
BgK N19A	97 ± 14 (7)[a]	1,590 ± 147 (5)	*0.39*	144 ± 20 (8)	*0.84*	121 ± 17 (10)	*0.54*	90.5 ± 6 (9)	*0.53*	1,170 ± 193 (3)	*0.34*
BgK S23A	920 ± 160 (4)	ND	ND	ND	ND	ND	ND	ND	ND	3,640 ± 372 (3)	*0.99*
BgK Q24A	44 ± 3.7 (4)	ND	ND	ND	ND	ND	ND	ND	ND	548 ± 176 (3)	*0.32*
BgK K25A	5,497 ± 2,548 (3)	9,090 ± 1,108 (3)	*0.93*	5,600 ± 2,200 (4)	*1.06*	13,000 ± 7,000 (4)	*0.91*	7,300 ± 207 (3)	*0.73*	2,133 ± 66 (2)	*2.33*
BgK Y26A	210 ± 35 (13)[a]	1,206 ± 261 (5)	*0.21*	253 ± 54 (7)	*0.96*	532 ± 66 (3)	*0.95*	123 ± 8.7 (6)	*0.26*	1,265 ± 164 (4)	*0.75*

[a] Values were determined by dose-response experiments, otherwise, they were deduced from blockade of the current by certain concentrations of toxin that allowed the calculation of K_d values.
[b] ND, not done.

FIG. 3. **Coupling energies from the double mutant cycles.** Coupling energies were calculated as described in the text. The values > 0.7 kcal·mol^{-1} are shown by the *dark cylinders*.

TABLE II
Structural statistics of the models of BgK/S5-S6 region of Kv1.1 (averaged over the 100 models)

Number of restraints[a]	6
Number of models	10
Violations of the restraints	*Number of structures*
> 1 Å	0
> 0.5 Å	1
Average distances between the residues on which distance restraints were applied[a]	
Phe^{6}-Tyr_D^{379}	5.2 Å
Asn^{19}-Ser_C^{357}	6.3 Å
Ser^{23}-Tyr_D^{379}	4.8 Å
Tyr^{26}-Ser_D^{357}	7.2 Å
Tyr^{26}-Asp_D^{361}	7.6 Å
Tyr^{26}-Tyr_D^{379}	6.5 Å
Cα r.m.s.d.	
Over the starting model of Kv1.1 (fixed regions[b])	1.8 Å
Over the average model flexible region of Kv1.1[b]	2–5 Å
BgK	1.7 Å
Buried surface	1,040 ± 64 Å^2
Energies	
E_{Tot}	− 3,593 ± 18 kcal·mol^{-1}
E_{bond}	61 ± 0.7 kcal·mol^{-1}
E_{angle}	418 ± 6 kcal·mol^{-1}
$E_{improper}$	77 ± 2 kcal·mol^{-1}
$E_{Van\ der\ Waals}$	− 3,326 ± 19 kcal·mol^{-1}
E_{elec}[c]	− 1,146 ± 9 kcal·mol^{-1}
$E_{distance\ constraint}$[d]	1.9 ± 1 kcal·mol^{-1}

[a] 6 + 1, −3 Å between the residues (BgK-Kv1.1 subunit): Phe^{6} (cycle atoms)-Tyr_A^{379}, Asn^{19}(Nδ2/Oδ1)-Ser_C^{357}(Oγ), Ser^{23}(Oγ/Hγ)-Tyr_D^{379}(Oη), Tyr^{26}(Oη)-Ser_D^{357}(Oγ), Tyr^{26}(Oη)-Asp_D^{361}(Oδ) and Y26(cycle atoms)-Tyr_D^{379}(cycle atoms).
[b] Fixed regions of the channel, residues 325–345 and 365–409; flexible regions of the channel, residues 350–360.
[c] Electrostatic energy was calculated with a dielectric constant equal to 10.
[d] The energy constant for distance restraint was set to 3 kcal · mol.$^{-1}$

Some fluctuations in the turret region were allowed during calculations of the models of the complex BgK/S5-S6 region of Kv1.1. The reason for that was based on a previous molecular dynamic of the KcsA channel in a bilayer membrane which showed the flexibility of this region (35). These fluctuations were neither seen in the x-ray structure (36), as this region is involved in protein-protein crystal contacts, nor in the more recent structure solved at 2 Å resolution (22), where KcsA is complexed with a Fab fragment, via the turret region. How-

ever, comparison of the two structures reveals for the turret region slight differences on Cα positions and large variation of the χ1 angles. Furthermore, recent docking studies also suggest some structural differences between bacterial and mammalian channels, in particular in the region containing residues 53 and 56 (using the *KcsA* numbering) (19).

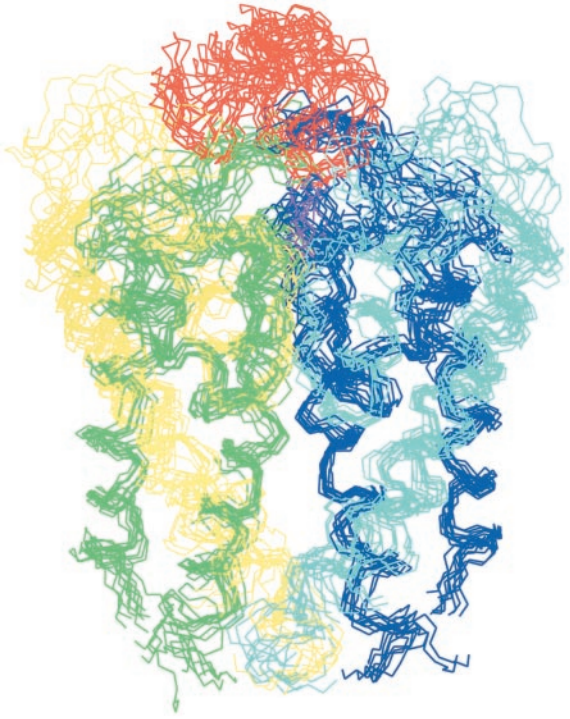

FIG. 4. **Structures of the complex BgK/S5-S6 region of Kv1.1.** Structures of the 10 complexes, superimposed on the fixed region of the channel (325–345, 365–409), are shown. The subunits of the channel are colored *yellow* (subunit A), *blue* (subunit B), *cyan* (subunit C), and *green* (subunit D). BgK is colored *red*, and the side chain is of Lys^{25} is shown and colored *magenta*.

In fine, we considered 10 complex structures whose structural statistics are shown in Table II. These structures converged (Fig. 4); the mean Cα r.m.s.d. for the docked BgK is 1.7 Å around the average structure of the complex. Residues of BgK whose relative solvent accessible surface area in the complex is less than 30% and for which difference between their relative solvent accessible surface area alone and complexed with the channel is more than 30% were defined as forming the binding site: it includes 14 residues (Arg^3, Trp^5, Phe^6, Lys^7, Glu^8, His^{13}, Thr^{22}, Ser^{23}, Gln^{24}, Lys^{25}, Tyr^{26}, Arg^{27}, Ala^{28}, and Asn^{29}). To compare this binding site to the functional sites of BgK, we identify the residues of BgK important for binding to Kv1.1, Kv1.2, and Kv1.6, using binding experiments (Ref. 37 and Fig. 5). In agreement with previous results (24), these binding sites contain three common residues: Ser^{23}, Lys^{25}, and Tyr^{26}. In addition to these residues, four residues were found be important for BgK binding to Kv1.1 (change in free energy of binding $\Delta\Delta G$ upon alanine substitution >1 kcal·mol^{-1}): Arg^3, Lys^7, His^{13}, Asn^{19}. Therefore, the functional site of BgK for binding to Kv1.1 contains seven residues. Interestingly, all these residues but Asn^{19} are included in the binding site. However, Asn^{19} is at the border of this interface (Fig. 6*A*), and even so, the difference between its relative solvent accessible surface area alone or complexed is 20%. The remaining eight residues that form the binding site are: Asn^{29}, which could not be definitively identified as functionally important because of structural perturbations induced by its alanine substitution; Glu^8, Thr^{22}, Gln^{24}, and Ala^{28}, located at the edge of the binding site, which have not been identified as important residues for binding to Kv1.2 and Kv1.6; and Trp^5, Phe^6, and Arg^{27}, which are important for BgK binding to other Kv1 subtypes (Kv1.2 and Kv1.6) (Fig. 6*A*).

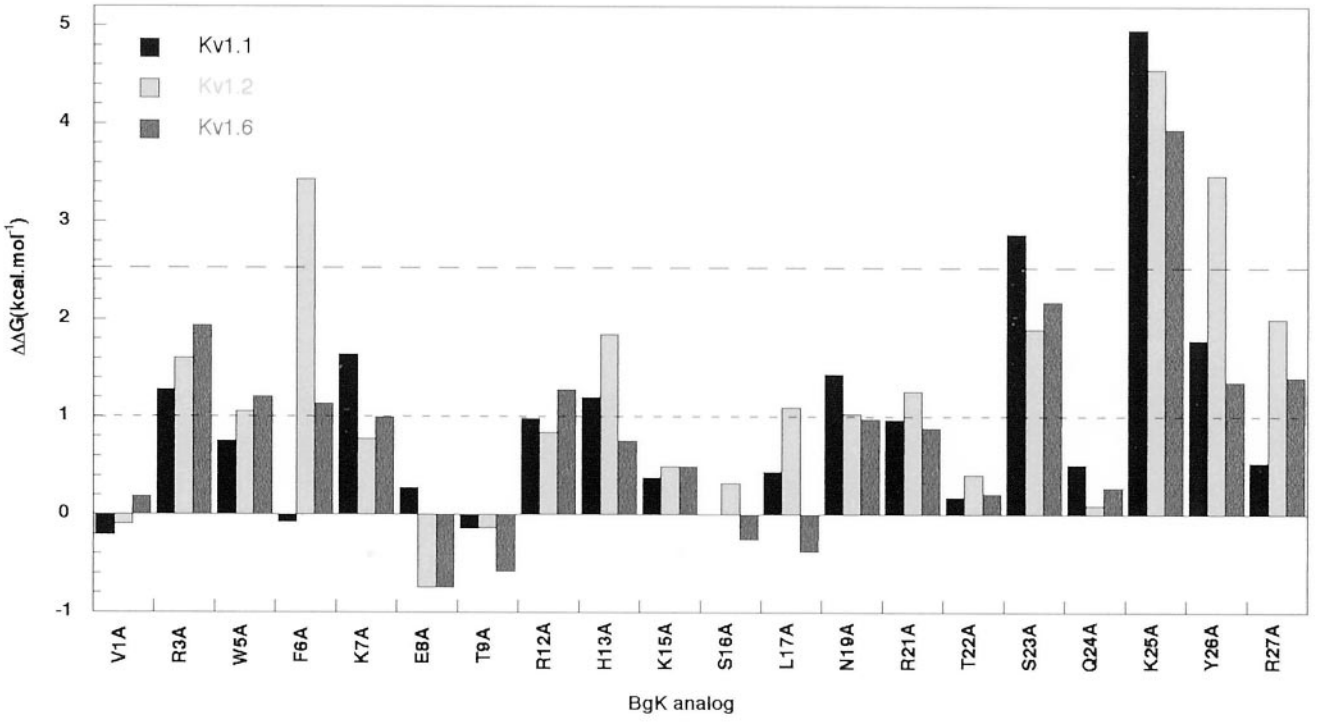

FIG. 5. **Functional mapping of Bgk on Kv1.1, Kv1.2, and Kv1.6.** The effects of alanine substitutions in BgK on affinity for Kv1 channels were measured by competition experiments; membranes prepared from HEK-293 or tsA-201 cells producing hKv1.1, hKv1.2, and hKv1.6 were incubated with 10 pM ^{125}I-α-DTX (hKv1.1, hKv1.2) or 8–10 pM ^{125}I-BgK(W5Y/Y26F) (hKv1.6) in the absence or presence of increasing concentrations of BgK analogs. The CD spectra of the analogs were identical to that of BgK except for N29A, K32A, T33A, K35A, and L36A (24). Therefore the functional effects associated with these substitutions were not considered.

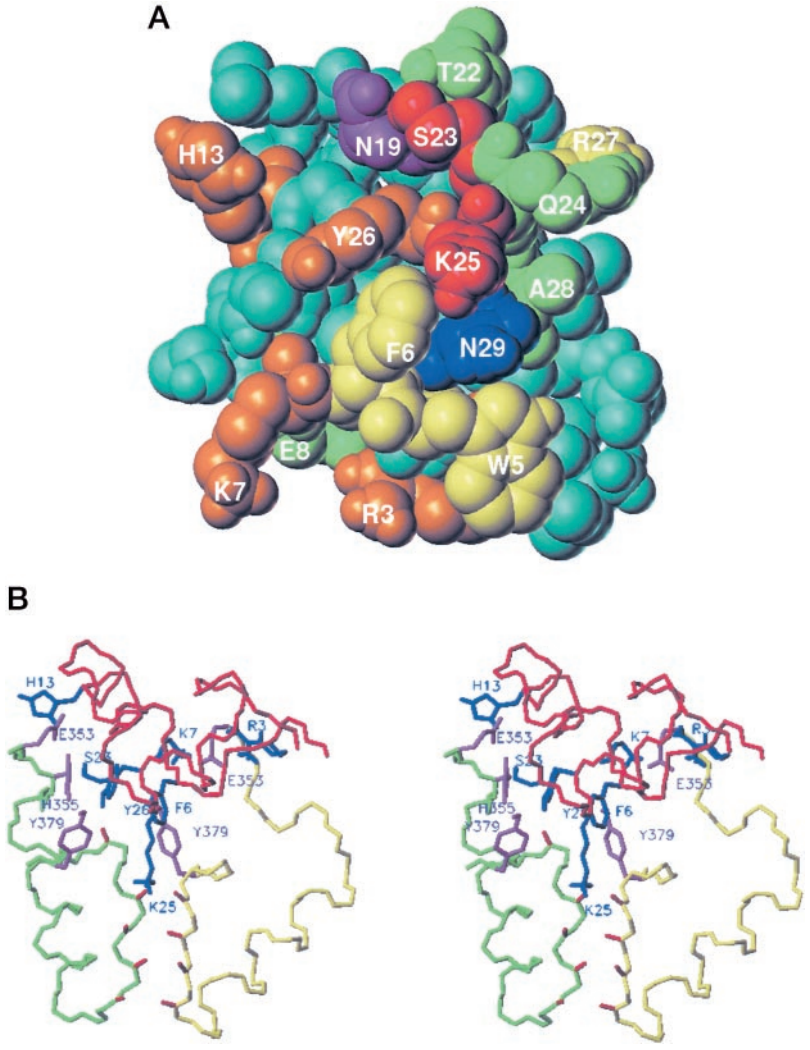

FIG. 6. **Interface of BgK in the model of BgK/S5-S6 region of Kv1.1 and interactions.** *A*, the 14 residues of the interface (as defined in the text) are colored as follows: *red*, hot spots for binding to Kv1.1 ($\Delta\Delta G$ upon alanine substitution >2.5 kcal·mol^{-1}); *orange*, less important residues ($\Delta\Delta G$ >1 kcal·mol^{-1}); *yellow*, residues important for BgK binding to Kv1.2 and Kv1.6; *green*, residues not important for binding to Kv1.1, Kv1.2, and Kv1.6. Asn^{19}, which is important to Kv1.1 but which is not in the interface, is colored *magenta*, and Asn^{29}, whose functional role could not be defined, since its alanine substitution induces structural perturbations, is colored *blue*. *B*, backbone is colored *red* for BgK, *green* for Kv1.1 subunit A, and *yellow* for subunit D (residues 353–379). The side chains are colored *magenta* for Kv1.1 residues and *blue* for BgK residues. Carbonyl oxygen atoms from the selectivity filter are shown and colored *red*.

The two most important residues for binding to Kv1.1, Lys^{25} and Ser^{23} (Fig. 5), are central in the interface (Fig. 6*A*). The side chain of Lys^{25} is projecting into the channel pore (Figs. 4 and 6*B*) and its extremity (r.m.s.d. over the average model: 2.0 Å for the Nζ) is located 1 Å above the plane defined by the four carbonyl oxygens of Tyr^{375}, at 3 Å from the potassium binding site S1 (defined as the center of gravity of the eight carbonyl oxygens of residues 374–375) at a position close to the potassium binding site S0, as defined in Ref. 26 (Fig. 6*B*). No interaction has been identified for the side chain of Ser^{23}, although its hydroxyl could be involved in a hydrogen bond with the hydroxyl of Tyr$^{379}{}_{D}$ (Fig. 6*B*). The third important residue for BgK binding to Kv1.1 is Tyr^{26}, which is also central in the interface (Fig. 6*A*). It interacts with several regions of the channel; its cycle is located in a pocket between the cycles of Tyr$^{379}{}_{A,D}$ from the loop connecting the selectivity filter to the transmembrane helix and is stacked on the imidazol ring of His$^{355}{}_{D}$ from the turret (Fig. 6*B*). The hydroxyl of Tyr^{26} is likely to be involved in an hydrogen bond with the carbonyl oxygen of Asp$^{377}{}_{D}$. However, this should not contribute much to the interaction energy, since replacing Tyr^{26} by a phenylalanine residue does induce only a small change in free energy of binding ($\Delta\Delta G$ = 0.68 kcal·mol^{-1}) (data not shown). Residues Arg^{3}, Lys^{7}, His^{13}, and Asn^{19} also contribute to the binding of BgK to Kv1.1; they are at the periphery of the interface (Fig. 6*A*). Residues Arg^{3} and Lys^{7} interact with Glu$^{353}{}_{A}$, whereas His^{13} interacts with Glu$^{353}{}_{D}$ (Fig. 6*B*). No interaction implicating residue Asn^{19} was identified. The cycle of residue Phe^{6}, which is important for binding to Kv1.6 and Kv1.2, but not for Kv1.1 (Fig. 5), is located in a pocket between the cycles of Tyr^{379} from two adjacent subunits A and D (Fig. 6*B*). Thus, both cycles of residues Phe^{6} and Tyr^{26} fill this pocket, Tyr^{26} being closer to Tyr$^{379}{}_{D}$, while Phe^{6} is closer to Tyr$^{379}{}_{A}$.

DISCUSSION

We determined the structure of the complex BgK-S5-S6 region of Kv1.1, using distance restraints deduced from double mutant cycle analysis. To estimate the atomic resolution of this complex, several structures were calculated. All 10 structures, which were obtained by flexible docking, are geometrically and energetically correct with a negative van der Waals energy, and the buried surface area (~1,000 Å^2) is in agreement with those observed typically for a protein-protein interface (38). The r.m.s.d. on the Cα atoms of the docked BgK is equal to 1.7 Å, indicating that the position of the ligand is well defined.

This structure provides a molecular basis for understanding how BgK binds to different Kv1 channels. Indeed, BgK binds with similar affinities to Kv1.1, Kv1.2, and Kv1.6 and with a lower affinity to Kv1.3 (18). The functional sites of BgK for the these channels are very similar and contain a common core of three hot spot residues: the dyad residues Lys^{25} and Tyr^{26} and Ser^{23} (Refs. 24 and 37; Fig. 5). Furthermore, the different Kv1 subtypes are also highly analogous (83% identity) in the P-region. Thus, the topologies of the different BgK-Kv1 channel complexes are likely to be very similar.

The general organization of functional residues in the binding site of BgK to Kv1.1 has been described in many protein-protein interfaces (38, 39): the three important residues Ser^{23}, Lys^{25}, and Tyr^{26} are central and surrounded by less important residues, solvent-accessible. The major determinant for BgK binding to Kv1.1 is formed by electrostatic interactions between the extremity of Lys^{25} side chain and carbonyl oxygen atoms of residues from the channel selectivity filter (Fig. 6*B*). Since these interactions involve residues from the most conserved region of Kv1 channels, they are likely to be conserved in all complexes Kv1-BgK. The second determinant for BgK binding to Kv1.1 is formed by hydrophobic interactions between Kv1.1 Tyr^{379} residue whose side chain is protruding in the channel vestibule and two BgK residues: the hot spot dyad residue Tyr^{26} and Phe^{6} (Fig. 6*B*). These hydrophobic interactions surround the Lys^{25} side chain and are thought to be important to strengthen the electrostatic interactions between this lysine and the oxygen atoms from the selectivity filter residues, by allowing their exclusion from solvent. Although Tyr^{379} is a variable residue, as far as the corresponding residue in other channels is hydrophobic, the hydrophobic nature of these interactions can be reproduced in other complexes. The importance of these hydrophobic interactions is confirmed by the correlation between the nature of residue 379 in Kv1 channels and the affinity of BgK for these channels. Indeed, BgK binds more tightly to Kv1.1, Kv1.2, and Kv1.6 in which residue 379 is either a tyrosine or a valine than to Kv1.3 where this residue is less hydrophobic (histidine) (18) (Fig. 1). Furthermore, replacement of Tyr^{379} in Kv1.1 by a histidine residue decreases the affinity of BgK (Table I), and conversely, replacement in Kv1.3 of His^{379} (using Kv1.1 numbering) by a tyrosine residue enhances the affinity of BgK to a level comparable with that for Kv1.1 (18). Moreover, the differential effect of substitution F6A in BgK on its affinity for Kv1 channels (Fig. 5), which was shown to depend on the nature of residue 379 (18), also enlightens the importance of hydrophobic interactions involving the channel residue 379 (Fig. 6*B*). Indeed, we can correlate this effect to the capacity of residue 6 of BgK to make hydrophobic interactions with residue 379. In the complex BgK-Kv1.1, Phe^{6} is located in a pocket between two Tyr^{379}. We propose that an alanine at position 6 in BgK should still be able to make some hydrophobic interactions with Tyr^{379} (Kv1.1 and Kv1.6), whereas this could not be possible with the smaller residue equivalent in Kv1.2 (valine). Therefore, we showed that the residues from the functional core used by BgK to bind different Kv1 channels are likely to be involved in conserved important interactions, implicating both conserved and variable residues from the channels. Such a conservation of interactions involving interplay between conserved and variable residues has been described in other protein-protein interaction studies (2, 40).

Other toxin-potassium channel systems have been characterized. Despite the unrelated structures of these toxins, their binding sites all contain a functional dyad composed of a lysine and a hydrophobic residue (3). Structures of scorpion toxins and of ShK, a sea anemone toxin related to BgK, complexed with Kv1 channels (19, 41)[2] have been calculated using a restraint between the dyad lysine and a conserved tyrosine from the selectivity filter, identified by double mutant cycle analysis (30, 42). Interestingly, although we did not apply any restraint on the BgK dyad lysine to calculate our structure, its configuration in the complex is similar to those described in the latter structures, confirming a common role for scorpion and sea anemone toxins' dyad lysine. Therefore, the convergent evolution that led to the concomitant conservation in both sea anemone and scorpion potassium channel blockers of a functional dyad formed by lysine and a hydrophobic residue may reflects a convergent binding solution based on a crucial interplay between two conserved set of interactions. These are (i) specific electrostatic interactions between carbonyl oxygen atoms of the channel's selectivity filter residues and the extremity of the dyad lysine side chain, which are reinforced by exclusion from solvent (ii) by nonspecific hydrophobic interactions between nonconserved residues of the channel and the hydrophobic dyad residue.

Acknowledgments—We are grateful to Thomas Felix and Katharina Ruff for technical assistance and to Benoît Roux for providing unpublished data.

[2] B. Roux, personal communication.

REFERENCES

1. Kleanthous, C., and Pommer, A. J. (2000) in *Protein-Protein Recognition*, (Kleanthous, C., ed) pp. 280–311, Oxford University Press, Oxford, UK
2. Delano, W. L., Ultsch, M. H., de Vos, A. M., and Wells, J. A. (2000) *Science* **287,** 1279–1283
3. Ménez, A., Servent, D., and Gasparini, S. (2002) in *Perspectives in Molecular Toxinology* (Ménez, A., ed) Vol. 10, pp. 175–202, John Wiley and Sons Ltd., Chichester, UK
4. Stocker, M., Pongs, O., Hoth, M., Heinemann, S., Stühmer, W., Schröter, K.-H., and Ruppersberg, J. P. (1991) *Proc. R. Soc. Lond. B Biol. Sci.* **245**, 101–107
5. Hurst, R. S., Busch, A. E., Kavanaugh, M. P., Osborne, P. B., North, R. A., and Adelman, J. P. (1991) *Mol. Pharmacol.* **40,** 572–576
6. Goldstein, S. A., and Miller, C. (1993) *Biophys. J.* **65,** 1613–1619
7. MacKinnon, R., Heginbotham, L., and Abramson, T. (1990) *Neuron* **5,** 767–771
8. Gross, A., Abramson, T., and MacKinnon, R. (1994) *Neuron* **13,** 961–966
9. Kim, M., Baro, D. J., Lanning, C. C., Doshi, M., Farnham, J., Moskowitz, H. S., Peck, J. H., Olivera, B. M., and Harris-Warrick, R. M. (1997) *J. Neurosci.* **17,** 8213–8224
10. Shon, K. J., Stocker, M., Terlau, H., Stühmer, W., Jacobsen, R., Walkern, C., Grilley, M., Watkins, M., Hillyard, D. R., Gray, W. R., and Olivera, B. (1998) *J. Biol. Chem.* **273**, 33–38
11. Garcia, E., Scanlon, M., and Naranjo, D. (1999) *J. Gen. Physiol.* **114,** 141–157
12. Garcia, M. L., Gao, Y. D., McManus, O. B., and Kaczorowski, G. J. (2001) *Toxicon* **39,** 739–748
13. Dauplais, M., Lecoq, A., Song, J., Cotton, J., Jamin, N., Gilquin, B., Roumestand, C., Vita, C., de Medeiros, C. L. C., Rowan, E. G., Harvey, A. L., and Ménez, A. (1997) *J. Biol. Chem.* **272,** 4302–4309
14. Gasparini, S., Danse, J. M., Lecoq, A., Pinkasfeld, S., Zinn-Justin, S., Young, L. C., de Medeiros, C. L. C., Rowan, E. G., Harvey, A. L., and Ménez, A. (1998) *J. Biol. Chem.* **273,** 25393–25403
15. Savarin, P., Guenneugues, M., Gilquin, B., Lamthanh, H., Gasparini, S., Zinn-Justin, S., and Ménez, A. (1998) *Biochemistry* **37,** 5407–5416
16. Rauer, H., Pennington, M., Cahalan, M., and Chandy, K. G. (1999) *J. Biol. Chem.* **274,** 21885–21892
17. Jacobsen, R. B., Dietlind Koch, E., Lange-Malecki, B., Stocker, M., Verhey, J., Van Wagoner, R. M., Vyazovkina, A., Olivera, B. M., and Terlau, H. (2000) *J. Biol. Chem.* **275,** 24639–24644
18. Racapé, J., Lecoq, A., Romi-Lebrun, R., Liu, J., Kohler, M., Garcia, M. L., Ménez, A., and Gasparini, S. (2002) *J. Biol. Chem.* **277,** 3886–3893
19. Wrisch, A., and Grissmer, S. (2000) *J. Biol. Chem.* **275**, 39345–3935320
20. Hamill, O. P., Marty, E., Neher, E., Sakmann, B., and Sigworth, F. J. (1981) *Pflügers Arch.* **391,** 85–100
21. Sali, A., Potterton, L., Yuan, F., van Vlijmen, H., and Karplus, M. (1995) *Proteins* **23,** 318–326
22. Zhou, Y., Morais-Cabral, J. H., Kaufman, A., and MacKinnon, R. (2001) *Nature* **414**, 43–48
23. Savarin, P., Romi-Lebrun, R., Zinn-Justin, S., Lebrun, B., Nakajima, T., Gilquin, B., and Ménez, A. (1999) *Protein Sci.* **8,** 2672–2685
24. Alessandri-Haber, N., Lecoq, A., Gasparini, S., Grangier-Macmath, G., Jacquet, G., Harvey, A. L., de Medeiros, C. L. C., Rowan, E. G., Gola, M., Ménez, A., and Crest, M. (1999) *J. Biol. Chem.* **274**, 35653–35661
25. Morais-Cabral, J. H., Zhou, Y., and MacKinnon, R. (2001) *Nature* **414,** 37–42
26. Bernèche, S., and Roux, B. (2001) *Nature* **414,** 73–76
27. Brünger, A. T. (1992) *X-PLOR, A system for X-ray cristallography and NMR,* version 3.1, Yale University Press, New Haven, CT
28. Kalman, K., Pennington, M. W., Lanigan, M. D., Nguyen, A., Rauer, H., Mahnir, V., Paschetto, K., Kem, W. R., Grissmer, S., Gutman, G. A., Christian, E. P., Cahalan, M. D., Norton, S., and Chandy, K. G. (1998) *J. Biol. Chem.* **273,** 32697–32707
29. Imredy, J. P., and MacKinnon, R. (2000) *J. Mol. Biol.* **296,** 1283–1294
30. Ranganathan, R., Lewis, J. H., and MacKinnon, R. (1996) *Neuron* **16,** 131–139
31. Jäger, H., Rauer, H., Nguyen, A. N., Aiyar, J., Chandy, K. G., and Grissmer, S. (1998) *J. Physiol.* (*Lond.*) **506,** 291–301
32. Carter, P. J., Winter, G., Wilkinson, A. J., and Fersht, A. R. (1984) *Cell* **38,** 835–840
33. Schreiber, G., and Fersht, A. R. (1995) *J. Mol. Biol.* **248**, 478–486

34. Roisman, L. C., Piehler, J., Trosset, J. Y., Scheraga, H. A., and Schreiber, G. (2001) *Proc. Natl. Acad. Sci. U. S. A.* **98,** 13231–13236
35. Bernèche, S., and Roux, B. (2000) *Biophys. J.* **78,** 2900–2917
36. Doyle, A. D., Morais Cabral, J., Pfuetzner, R. A., Kuo, A., Gulbis, J. M., Cohen, S. L., Chait, B. T., and MacKinnon, R. (1998) *Science* **280,** 69–77
37. Racapé, J. (2001) *Identification and Analysis of Molecular Determinants Used by Animal Toxins to Bind Kul Channels.* PhD thesis, Université Paris-Sud XI, Paris
38. Chakrabarti, P., and Janin, J. (2002) *Proteins* **47,** 334–343
39. Bogan, A. A., and Thorn, K. S. (1998) *J. Mol. Biol.* **280,** 1–9
40. Kühlmann, U. C., Pommer, A. J., Moore, G. R., James, R., and Kleanthous, C. (2000) *J. Mol. Biol.* **301,** 1163–1178
41. Rauer, H., Lanigan, M. D., Pennington, M. W., Aiyar, J., Ghanshani, S., Cahalan, M. D., Norton, R. S., and Chandy, K. G. (2000) *J. Biol. Chem.* **275**, 1201–1208
42. Aiyar, J., Withka, J. M., Rizzi, J. P., Singleton, D. H., Andrews, G. C., Lin, W., Boyd, J., Hanson, D. C., Simon, M., and Dethlefs, B. (1995) *Neuron* **15,** 1169–1181

Structure of the BgK-Kv1.1 Complex Based on Distance Restraints Identified by Double Mutant Cycles: MOLECULAR BASIS FOR CONVERGENT EVOLUTION OF Kv1 CHANNEL BLOCKERS

Bernard Gilquin, Judith Racapé, Anja Wrisch, Violeta Visan, Alain Lecoq, Stephan Grissmer, André Ménez and Sylvaine Gasparini

J. Biol. Chem. 2002, 277:37406-37413.
doi: 10.1074/jbc.M206205200 originally published online July 19, 2002
